JCB Article

Coalignment of plasma membrane channels and protrusions (fibripositors) specifies the parallelism of tendon

Elizabeth G. Canty, Yinhui Lu, Roger S. Meadows, Michael K. Shaw, David F. Holmes, and Karl E. Kadler

Wellcome Trust Centre for Cell-Matrix Research, School of Biological Sciences, University of Manchester, Manchester M13 9PT UK

The functional properties of tendon require an extracellular matrix (ECM) rich in elongated collagen fibrils in parallel register. We sought to understand how embryonic fibroblasts elaborate this exquisite arrangement of fibrils. We show that procollagen processing and collagen fibrillogenesis are initiated in Golgi to plasma membrane carriers (GPCs). These carriers and their cargo of 28-nm-diam fibrils are targeted to previously unidentified plasma membrane (PM) protrusions (here designated "fibripositors") that are parallel to the tendon axis and project into parallel channels between cells. The base of the fibripositor lumen (buried several microns within the cell) is a nucleation site of collagen fibrillogenesis. The tip of the fibripositor is the site of fibril deposition to the ECM. Fibripositors are absent at postnatal stages when fibrils increase in diameter by accretion of extracellular collagen, thereby maintaining parallelism of the tendon. Thus, we show that the parallelism of tendon is determined by the late secretory pathway and interaction of adjacent PMs to form extracellular channels.

Introduction

The ability of tendon to withstand repeated cycles of tensile force is largely attributable to the presence in the ECM of collagen fibrils that are indeterminate in length and exhibit large diameters. Moreover, the fibrils occur in strict parallel register. It is controversial how the parallelism of tendon arises and how long fibrils are deposited into the ECM. The fibrils, which comprise triple helical collagen molecules that are quarter staggered along the fibril long axis, exhibit a characteristic 67-nm axial periodicity (the '*D*-periodicity') and are readily observed by EM (Parry et al., 1978). They can be partially solubilized in cold or weak acidic buffers thereby producing a solution of collagen molecules. Upon warming and neutralizing the solutions, the collagen molecules spontaneously self-assemble to form elongated fibrils that exhibit the same *D*-periodicity as tissue fibrils (Kadler et al., 1996). Reconstituted fibrils form semi-rigid gels in which the fibrils exhibit no preferred orientation. Therefore, although the collagen molecule contains all the necessary sequence information to form *D*-periodic fibrils it lacks information to direct parallel alignment of fibrils, which suggests a cellular involvement in vivo. However, cells alone are insufficient to specify parallelism of the fibrils; tendon fibroblasts in culture do not assemble a functional tissue, despite synthesizing large amounts of collagen. Here, we tested the hypothesis that the secretory pathway of fibroblasts in situ determines the parallelism of collagen fibrils in tendon.

A primary function of the secretory pathway is to transport macromolecules from their site of synthesis in the ER to the plasma membrane (PM). A critically important node in this pathway is the Golgi complex with its associated TGN consisting of a complex network of anastomosing tubules (Rambourg et al., 1979). The TGN mediates the final modification of N-linked oligosaccharides to the complex form (Roth et al., 1985) and is involved in both the transport and sorting of membrane and secretory proteins (Griffiths and Simons, 1986; Taatjes and Roth, 1986; Orci et al., 1987). Previous works have shown that GFP fusion proteins

The online version of this article contains supplemental material.

Address correspondence to Karl E. Kadler, Wellcome Trust Centre for Cell-Matrix Research, School of Biological Sciences, University of Manchester, Michael Smith Building, Oxford Road, Manchester M13 9PT UK. Tel.: 44-161-275-5086. Fax: 44-161-275-1505. email: karl.kadler@man.ac.uk

Key words: 3-D reconstruction; collagen; fibril; GPC; procollagen

Abbreviations used in this paper: 3-D, three-dimensional; ADAMTS, a disintegrin and metalloprotease (reprolysin type) with thrombospondin motifs; BMP, bone morphogenetic protein; dpc, days post coital; GPC, Golgi to plasma membrane carrier; GPC^{+cf}, GPC containing one or more 67-nm periodic collagen fibrils; pCcollagen, a naturally occurring intermediate in the cleavage of procollagen to collagen that contains the C-propeptides and not the N-propeptides; PM, plasma membrane; pN-collagen, a naturally occurring intermediate in the cleavage of procollagen to collagen that contains the N-propeptides and not the C-propeptides.

are transported from the Golgi to the cell surface in tubular-saccular compartments, which travel along microtubules (Sciaky et al., 1997; Hirschberg et al., 1998; Toomre et al., 1999; Polishchuk et al., 2000; Puertollano et al., 2003). (In this paper, the authors distinguish between vesicles and compartments or carriers. The terms "compartment" and "carrier" refer to any membrane-bound transport container within the cell, regardless of its size, position, or function in the secretory pathway. The term "vesicle" refers to any compartment that is spherical or near spherical in shape, regardless of its size, position, or function in the secretory pathway.) These pleiomorphic Golgi to PM carriers (GPCs) can be 0.5–1.7 μm in length (Polishchuk et al., 2000) and have also been called transport containers (Toomre et al., 1999) and post-Golgi carriers (Hirschberg et al., 1998). A recent in vitro study has shown that exit from the TGN occurs by the formation of a tubular-reticular TGN domain that is a precursor structure to the release of tubular-saccular GPCs (Polishchuk et al., 2003).

Tendon fibrils are predominately comprised of collagen I, which is the most abundant collagen in vertebrates (Boot-Handford et al., 2003). It is synthesized in the ER as procollagen I, which comprises two proα1(I) chains and one proα2(I) chains folded into an uninterrupted 300-nm-long triple helix flanked by globular N- and C-propeptides. Procollagen molecules are too large to fit into conventional 60–80-nm transport vesicles and traverse the Golgi complex of these cells by cisternal maturation (Bonfanti et al., 1998). We were particularly interested to know if procollagen occurs in GPCs en route to the ECM. Of particular relevance to this question is that proteolytic cleavage of the N- and C-propeptides results in spontaneous collagen fibril formation. N-propeptide removal is catalyzed by the procollagen N-proteinases, which include a disintegrin and metalloprotease (reprolysin type) with thrombospondin motifs (ADAMTS)-2, -3, and -14 (Colige et al., 1997, 2002; Fernandes et al., 2001), whereas C-proteinase activity is possessed by all members of the tolloid family of zinc metalloproteinases including bone morphogenetic protein-1 (BMP-1; Scott et al., 1999). Both BMP-1 and ADAMTS-2 are activated by a furin-like proprotein convertase, and in the case of pro–BMP-1, activation has been shown to occur in the TGN (Leighton and Kadler, 2003; Wang et al., 2003). Furin itself undergoes autocatalytic activation and is thought to cycle between the TGN, the cell surface, and the endosomal system (Molloy et al., 1999; Thomas, 2002).

Seminal studies in the early 1980s by Birk, Trelstad, and coworkers (Trelstad and Hayashi, 1979; Birk and Trelstad, 1984, 1986) suggested that collagen fibrils occur in deep PM recesses and that the recesses increase in diameter at distances from the cell to accommodate fibril bundles. Evidence from EM autoradiography indicated that newly synthesized collagen molecules pass through these recesses en route to the ECM. However, recent findings that pro–BMP-1 is converted to BMP-1 in the TGN, as well as studies of GPCs in cultured cells, prompted us to relate these new observations to the description of fibril formation in embryonic tendon described by Trelstad and colleagues (see references above). Here, we show that GPCs are indeed present in embryonic tendon fibroblasts and that some GPCs contain 28-nm-diam collagen fibrils ($GPCs^{+cf}$). Moreover, $GCPs^{+cf}$ are targeted to novel PM protrusions, which we have termed "fibripositors" (fibril depositors). In addition, we show that procollagen can be converted to collagen within the confines of the cell membrane, which is consistent with the observation of collagen fibrils in some GPCs and the known intracellular activation of BMP-1. A novel observation was that fibripositors are always oriented along the tendon axis, which establishes a link between intracellular transport and the organization of the ECM. Interestingly, fibripositor formation is not a constitutive process in procollagen-secreting cells but occurs only during a narrow window of embryonic development when tissue architecture is being established.

Results

GPCs containing collagen fibrils occur in chick embryo tendon fibroblasts in vivo

Transverse (i.e., orthogonal to the tendon axis) sections of metatarsal tendons from chick embryos show membrane encapsulated collagen fibrils within the cytoplasm and bundles of fibrils in the ECM (not depicted), whereas longitudinal sections (i.e., parallel to the tendon long axis) showed GPCs containing cross-banded collagen fibrils ($GPCs^{+cf}$; Fig. 1 A). Three-dimensional (3-D) reconstructions were performed on six separate serial longitudinal sections from chick embryo leg tendons. The reconstructions showed the presence of $GPCs^{+cf}$, which varied in length up to ~2 μm, and associated small pleiomorphic membrane enclosures (Fig. 1 B). These $GPCs^{+cf}$ often were completely enclosed within the cell and the 67-nm banding pattern provided unequivocal identification of collagen fibrils. However, it was also shown that the $GPCs^{+cf}$ were reactive to a collagen I (triple helical region) antibody (Fig. 1 C).

The N- and C-propeptides of procollagen are cleaved in post-Golgi compartments

Pulse-chase experiments were performed on tendons from 13-d chick embryos. At this stage, the tendon fibroblasts synthesize mainly collagen I (Graham et al., 2000), which simplifies biochemical studies. To examine procollagen processing, pulse-chase experiments were performed on whole tendons using a 10-min pulse and 10–180-min chase. Using a differential extraction procedure (Fig. S1, available at http://www.jcb.org/cgi/content/full/jcb.200312071/DC1) we analyzed the ECM-resident proteins in a neutral high salt buffer and then the intracellular proteins in the same buffer supplemented with NP-40. The extracts were analyzed separately by SDS-PAGE and autoradiography. Trimeric type I procollagen (comprising two proα1(I) and one proα2(I) chain) can be processed by sequential removal of the N- and C-propeptides, and vice versa, producing eight different α-chains. In decreasing size order these are: proα1(I), pCα1(I), pNα1(I), proα2(I), pCα2(I), α1(I), pNα2(I), and α2(I). All eight bands can be seen in the 20-min chase NP-40 extract (Fig. 2 A). The migration of each chain was confirmed by comparison with radiolabeled procollagen digested with recombinant BMP-1, ADAMTS-2, or trypsin (unpublished data). The collagen chains were differentially distributed between the

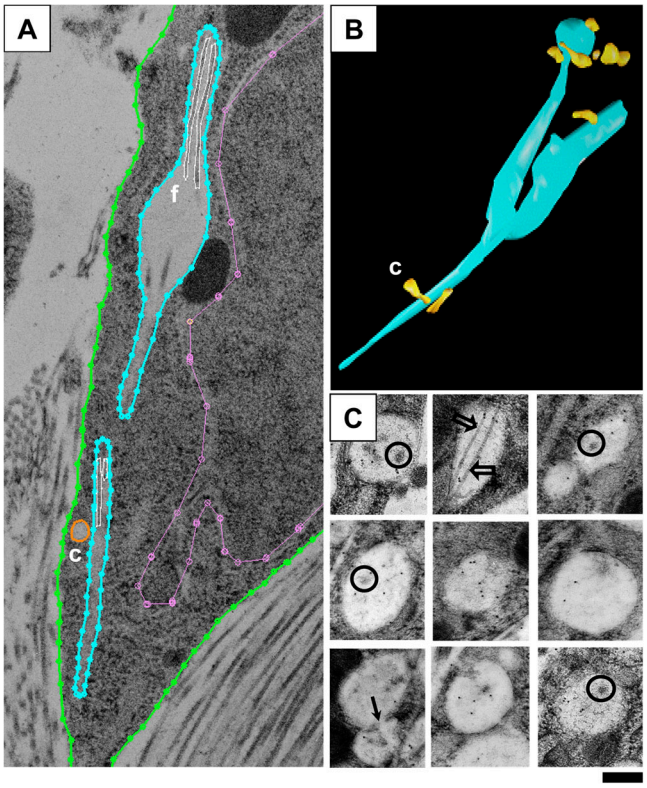

Figure 1. **GPCs in chick tendon fibroblasts contain collagen fibrils.** (A) A single longitudinal section of 10-d chick metatarsal tendon that was used to prepare one of the serial section 3-D reconstructions, showing part of one fibroblast. Green, the PM; blue, the membrane of an elongated GPC containing two collagen fibrils; f (and outlined in white), two intracellular fibrils; purple, the nuclear membrane; c (also outlined in orange), a small compartment positioned close to the fibril-containing GPC. (B) Serial section reconstruction (from longitudinal sections) of the GPC shown in A. Green, a solid surface 3-D representation of the GPC with associated small compartments (c). (C) Immunolocalization of collagen triple helices to GPCs using a colloidal-gold conjugated anti–rabbit IgG antibody recognizing a rabbit anti–type I collagen antibody. Closed arrow, two vesicles fusing; open circle, cross section of a collagen fibril; open arrow, cross-banded collagen fibrils. Bar, 100 nm.

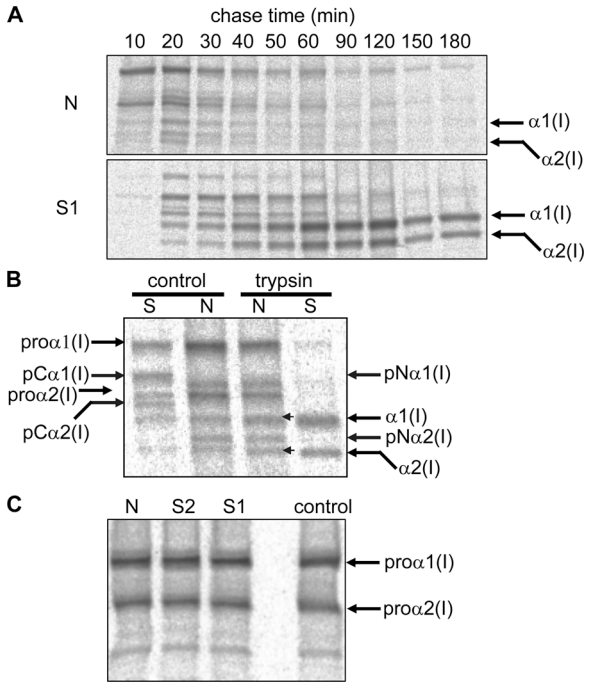

Figure 2. **Pulse-chase analysis of procollagen conversion by chick tendon fibroblasts in situ.** (A) Chick metatarsal tendons were incubated in medium containing [^{14}C]proline for 10 min and then in unlabeled medium for the times indicated. The tendons were successively extracted four times in buffer containing NaCl and then in a buffer containing NP-40. Autoradiography was used to display the labeled proteins in the chase samples. For brevity, only the first NaCl extract is shown. S1, the first salt extract. N, the NP-40 extract. (B) In a repeat experiment, the 30-min chase samples were incubated with trypsin and the labeled proteins displayed by autoradiography. Control, untreated; trypsin, trypsin treated; S, the first salt extract; N, the NP-40 solubilized proteins. The migration positions of the α-chains of procollagen, pCcollagen, pNcollagen, and collagen are indicated. (C) Tendons were subjected to a mock pulse chase (pulse 10 min, chase 60 min) in which no radiolabeled proline was added. They were then subjected to two salt (S1 and S2) extractions and a final NP-40 (N) extraction to which exogenous purified ^{14}C-labeled procollagen was added. The extracts were prepared for SDS-PAGE and the proteins analyzed by autoradiography. Procollagen remained uncleaved in the S and N samples.

NaCl (S1) and NP-40 (N) extracts (Fig. 2 A). Most of the ^{14}C-label was initially present in the NP-40 extract as procollagen. At later chase times, the NP-40 extract contained (a) procollagen; (b) a naturally occurring intermediate in the cleavage of procollagen to collagen that contains the N-propeptides and not the C-propeptides (pNcollagen); (c) a naturally occurring intermediate in the cleavage of procollagen to collagen that contains the C-propeptides and not the N-propeptides (pCcollagen); and (d) collagen, and the amount of label in the NP-40 extracts progressively decreased over the course of the experiment. In contrast, little ^{14}C-collagen was present in the NaCl extract at the start of the experiment. Procollagen, pCcollagen, and collagen occurred in the NaCl extract in the 20-min chase sample. The amount of procollagen and pCcollagen in the NaCl extract decreased during the chase such that after ~3 h all of the labeled protein was fully processed collagen I in the NaCl extract.

To gain further confidence that procollagen intermediates (e.g., pNcollagen and pCcollagen) occurred within the cell, we performed a pulse-chase experiment to produce a mixture of processed procollagen chains in both the NaCl and NP-40 extracts, and then digested the tendons with trypsin at 20°C for 30 min. At this temperature cellular protein export is prevented but trypsin can still degrade nontriple helical protein molecules. The tendons were then sequentially extracted. Analysis of the first NaCl extract (S1) and NP-40 extract (N) indicated that whereas the salt extractable material was clearly converted to collagen by trypsin, the detergent extractable material was protected from trypsin digestion (Fig. 2 B). This shows that material that is accessible to salt extraction buffer can also be accessed by trypsin, whereas compartments that can only be solubilized using NP-40 detergent are inaccessible to trypsin.

To confirm that cleavage of procollagen did not occur during the extraction procedure, tendons were subjected to the same extraction protocols as above but in the presence of partially purified ^{14}C-labeled procollagen. No processing of

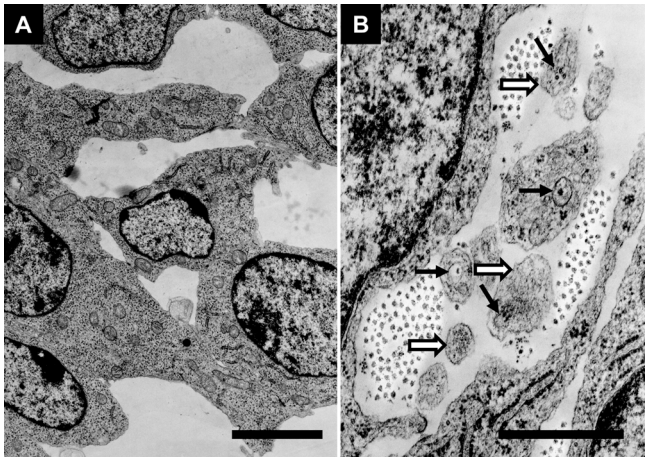

Figure 3. **Onset of fibripositor formation in mouse tail at 14.5 dpc.** (A) EM of tail tendon from a 13.5-d embryonic mouse showing predifferentiated fibroblasts with no obvious Golgi apparatus. Note the absence of collagen fibrils in the intercellular spaces. Bar, 500 nm. (B) EM of the proximal region of the tail from a 14.5-d embryonic mouse. Spaces between cells contain collagen fibrils in PM protrusions (open arrows), some of which contain collagen fibrils contained within lumen (closed arrows). Bar, 500 nm.

proα1(I) and proα2(I) chains occurred (Fig. 2 C), indicating that the labeled procollagen in the pulse-chase experiment must have been processed before extraction. To further confirm that intracellular collagen molecules could only be removed by extraction with buffer containing NP-40, pulse-chase experiments were performed in the presence of α,α-dipyridyl and brefeldin A. These treatments are both known to result in the accumulation of procollagen within the ER. Two successive NaCl extractions (S1 and S2) were performed before the NP-40 extraction (N), which was found to contain only unprocessed procollagen (unpublished data). These results are consistent with cleavage of procollagen to collagen occurring in post-Golgi compartments and the results of EM showing collagen fibrils in GPCs^{+cf}.

Appearance of PM protrusions coincides with onset of post-Golgi collagen fibril polymerization in 14.5-d mouse tail tendon

Transverse sections through the presumptive tail tendon of 13.5 dpc (days post coital) mouse embryos showed closely packed and apparently undifferentiated cells, which lacked evidence of GPCs^{+cf} or a fibrillar ECM (Fig. 3 A). However, cells in the proximal region of tails from 14.5 dpc embryos were loosely packed and had large extracellular spaces that contained numerous collagen fibrils. Cellular projections (Fig. 3 B, open arrows) were an obvious feature at this stage of development. Some of the projections contained tubular carriers in which collagen fibrils were clearly visible (Fig. 3 B, closed arrows). Analysis of the distal region of the same tails showed spaces between cells and a conspicuous absence of collagen fibrils and cellular projections, indicating that the development of mouse tail tendon proceeds from the proximal to the distal end. Therefore, the occurrence of parallel collagen fibrils in the ECM coincided with the appearance of cellular projections having GPCs^{+cf}.

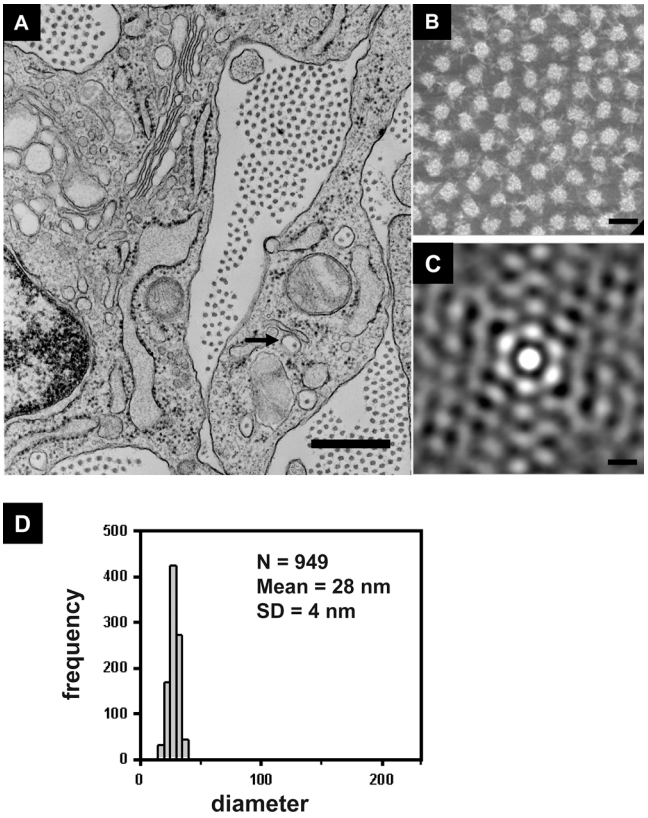

Figure 4. **Well-developed Golgi apparatus and active ECM assembly at 15.5 dpc.** (A) EM of tail tendon from 15.5 dpc mice showing well-developed Golgi complex, vacuolar TGN and membrane encapsulated collagen fibrils (closed arrow). Spaces between cells are occupied by narrow diameter collagen fibrils. Bar, 500 nm. (B) Electron microscope image of a transverse section showing part of a fibril bundle. Fibrils have a characteristic uniformity of diameter (mean diam = 28 nm; n = 949) and a uniformity of spacing (mean center to center spacing equals 58 nm; n = 380). Interconnections between the fibrils appear to stabilize the hexagonal packing arrangement. Bar, 50 nm. (C) Autocorrelation function of the image in (B) indicating a spatially ordered arrangement of fibrils in transverse section with an underlying near hexagonal array. Bar, 50 nm. (D) Histogram of fibril diameters.

Well-developed Golgi, parallel GPCs^{+cf} and parallel fibripositors in 15.5-d embryonic mouse tail tendon fibroblasts

By 15.5 dpc the mouse tail tendon contains an elaborate ECM containing parallel bundles of narrow collagen fibrils that are interconnected by filamentous strands (Fig. 4, A and B). Image analysis of collagen fiber bundles showed that the fibrils had a uniform diameter of 28 nm and were hexagonally packed with a mean fibril to fibril spacing of 58 nm (Fig. 4, B–D). The regular packing was disrupted only at sites where narrow fibril tips perturbed the center to center spacing but the fibril to fibril spacing of 58 nm was maintained. This packing arrangement, which has not previously been reported, is highly indicative of a cell-mediated mechanism of fibril deposition. The cells contained a well-defined Golgi complex and a highly vacuolar TGN (Fig. 4 A). There was an abundance of membrane encapsulated collagen fibrils within the cytoplasm of the same diameter as the extracellular fibrils (Fig. 4 A, arrow).

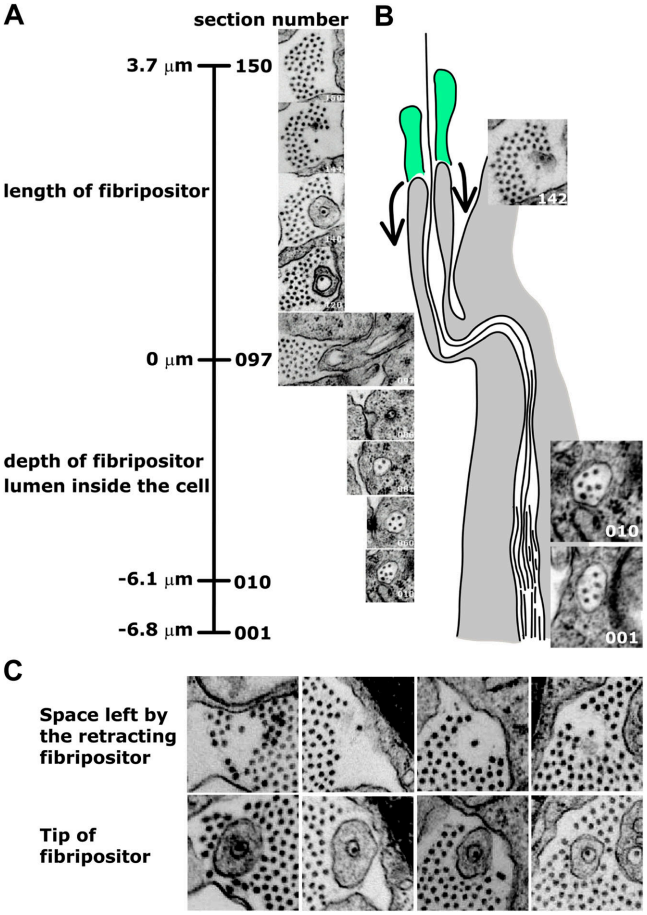

Figure 5. **Collagen fibrils can be traced from extracellular fibril bundles to deep within the cell.** (A) Transverse sections through a fibripositor and its intracellular lumen showing the path of individual collagen fibrils. A single fibril can be seen in a collagen bundle in the ECM, within the lumen of the fibripositor as it projects out from the cell, and within the lumen of the same fibripositor deep within the cell. Section numbers are indicated in white. A reference bar shows the section number, the depth of the fibripositor lumen within the cell, and the length of the fibripositor. (B) Schematic showing the transverse structure of a fibripositor. Arrows indicate proposed movement of the tip of the fibripositor as it retracts from the collagen bundle. (C) Gallery of images showing the space generated in the collagen bundle by the retracting fibripositor (top) and the corresponding tip of the fibripositor several sections below (or above) the space.

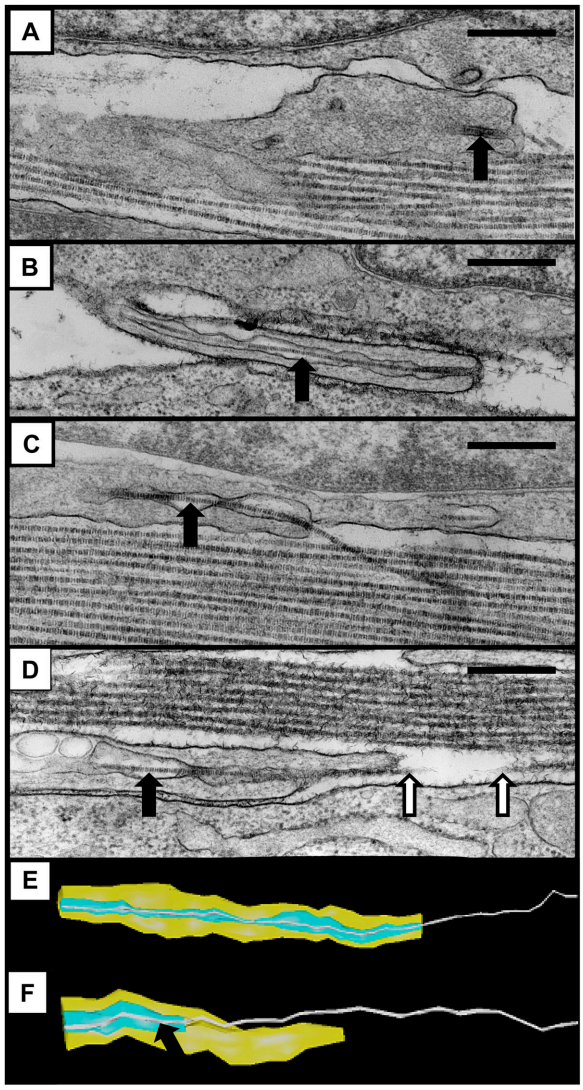

Figure 6. **Longitudinal structure of fibripositors from 15.5 dpc mouse tail tendons.** (A) Section through the proximal end of a fibripositor. (B and C) Collagen fibrils (closed arrow) are continuous from the ECM through the lumen of the fibripositor. The sidewalls of the lumen appear to grip collagen fibrils. (D) Intracellular compartments are often associated with the lumen of the fibripositor. A fibril is shown leaving and reentering the section (open arrow). (E and F) Cut-away views of two fibripositors from 3-D reconstructions. Closed arrow, collagen fibrils within lumen of fibripositor. Bars, 500 nm.

Five separate transverse serial section series were reconstructed (Video 1, available at http://www.jcb.org/cgi/content/full/jcb.200312071/DC1). These showed that the membrane-encapsulated collagen fibrils were aligned parallel to the tendon axis and that these carriers could either be enclosed within the cell ($GPCs^{+cf}$) or open to the extracellular space at one end (see Fig. 8 A). Closed $GPCs^{+cf}$ could either be located within membrane protrusions, as shown, or close to the Golgi complex (see Fig. 10 H). It was possible to trace the paths of individual fibrils through a transverse series from bundles in the ECM through the lumen of PM protrusions and into the main body of the cell, although most collagen fibrils exceeded the z-dimension of the reconstructions (Fig. 5). For descriptive purposes we have designated the PM protrusions "fibripositors". Occasionally it was possible to capture a fibripositor and its associated collagen fibrils in longitudinal section (Fig. 6, A–D). The fibripositors contained a lumen that extends several microns into the body of the cell. There were several common features of fibripositors: (a) in 85 fibripositors examined, 75 had a single fibril exiting the distal tip, five had two fibrils exiting, and five were closed at the distal end (i.e., contained a GPC containing one or more 67-nm periodic collagen fibrils [GPC^{+cf}] that was totally enclosed within the PM); (b) there was an S-shaped kink at the site where the fibripositor protruded from the main body of the cell; (c) the lumen was not uniform in diameter along the length of the fibripositor but often constricted to the diameter of a single fibril; (d) several fibrils could be located within the central lumen of the fibripositor,

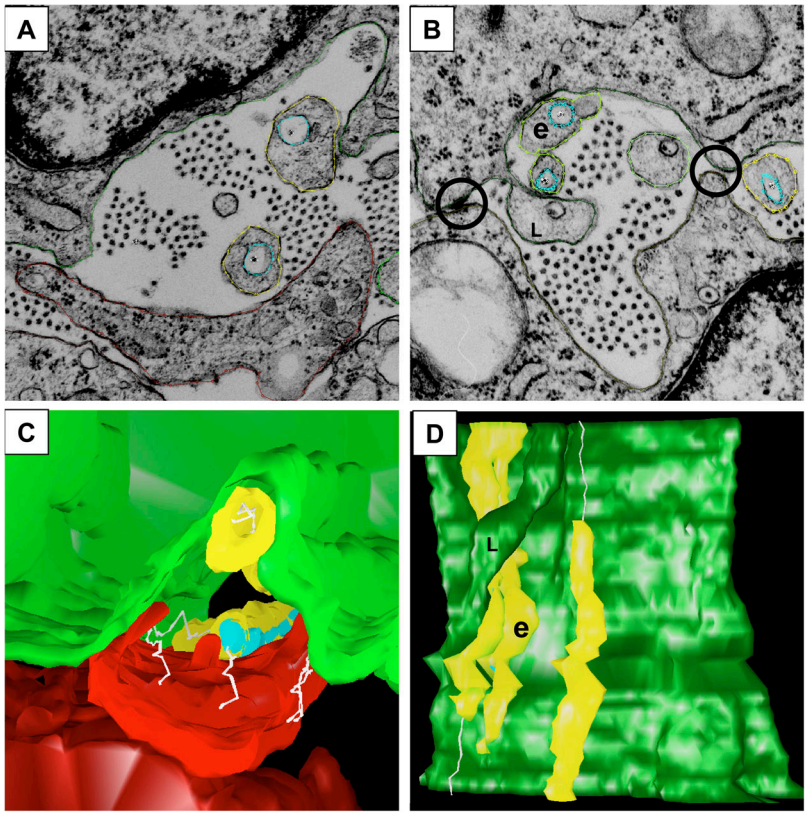

Figure 7. **Fibripositors project into cylindrical channels.** (A) EM showing a bundle of collagen fibrils between two cells (outlined in green and red). Fibripositors (outlined in yellow) project into a channel between the cells. One of the collagen fibrils in the bundle is highlighted in white. (B) The same channel as in A but at a different z-plane showing three fibripositors depositing fibrils to the bundle. A fibripositor located to the right-hand side of the image is shown depositing a fibril to a further fibril bundle. Cell–cell contacts are evident at the boundary of channels (open circles). e, enclosed fibripositors; L, leaflet of PM (see also D). The lumen of fibripositors are outlined in blue. (C) A plane taken through a 3-D reconstruction of the same cells as in A and B. The fibripositors and cells are rendered transparent to show the collagen fibrils (white). (D) Solid rendering of the cell outlined in green in A and B and viewed from one side. Two fibripositors (yellow) are shown, one of which is branched. One of the paired fibripositors deposits a fibril at the bottom of the reconstruction. A further fibripositor (yellow) is shown depositing a fibril at the top of the reconstruction. A leaflet (L) wraps around two fibripositors to define the boundaries of a small collagen fibril bundle. A closed fibripositor (e) is shown. Viewed from the side, the PM is seen as a wall of membrane running vertically along the long axis of the tendon.

i.e., within the main body of the cell; (e) the fibrils were often hexagonally packed within the lumen and had the same diameter as fibrils in the ECM; and (f) numerous short and very narrow fibrils occurred at the base of the fibripositor (Fig. 5 B, section 10).

Collagen fibrils are deposited by fibripositors into extracellular channels formed by adjacent fibroblasts

As cultured fibroblasts do not deposit parallel collagen fibrils, nor do they exhibit apparent GPCs^{+cf} or fibripositors it was not possible to use correlative microscopy techniques (including the use of GFP-tagged procollagen) to study the formation of fibripositors or the secretion of collagen fibrils. Therefore, to determine whether fibripositors deposit rather than remove fibrils from the ECM the serial sections were reexamined in further detail. In all examples in which a fibril could be seen exiting a fibripositor there was clear space around the fibril (a gallery of examples is shown in Fig. 5 C). In 3-D, the fibril was at the center (on axis) of a cylindrical space, which was identical in size and shape to the tip of the fibripositor. It is difficult to imagine how such a space could be generated by an encroaching fibripositor; therefore, it appears that the spaces are generated by retreating fibripositors. In addition, the fibrils deep within the fibripositor lumen were uniformly 28 nm in diameter, as were ECM fibrils, providing no evidence for fibril disassembly inside the fibripositors.

3-D reconstruction showed that tendon fibroblasts are roughly cylindrical in shape with their long axis parallel to the axis of the tendon. Moreover, the PM adopts a novel conformation to generate cylindrical channels that are parallel to the tendon-long axis. The fibripositors were also parallel to the long axis of the tendon and to the collagen fibril bundles (Figs. 6 and 7). Fibripositors projected into channels that were formed by close contacts between the PMs of adjacent cells (Fig. 7 B, open circles). The longitudinal axes of channels, which had smooth concave surfaces, were always parallel to the tendon-long axis (Fig. 7, A and B). Channels presumably provide a confined environment for the supramolecular organization of collagen fibrils into parallel bundles. Fibrils were observed exiting fibripositors in either direction along the tendon axis and branched fibripositors and branched lumen were also observed (Fig. 7 D).

The lumen of the fibripositor is accessible to HRP

To determine whether exogenous molecules such as nondetergent buffers and trypsin are able to penetrate into the lumen of the fibripositors in pulse-chase experiments, tendons from 13-d chick embryos were incubated in medium containing HRP. The presence of HRP was then detected using DAB, and transverse sections examined using EM. As shown in Fig. 8 B, electron dense material occurred in some fibripositors (closed arrowheads) whereas others remained clear (open arrowheads).

GPCs^{+cf} are absent during postnatal development despite active procollagen synthesis

Fibroblasts from the tails of 6-wk-old mice were stellate in cross section, surrounded by a dense matrix of collagen fibrils and lacked fibripositors or intracellular collagen fibrils (unpublished data). The fibrils had a diameter of 151 nm ($\pm$69; n = 521) and the distribution was broad (Fig. 9 C).

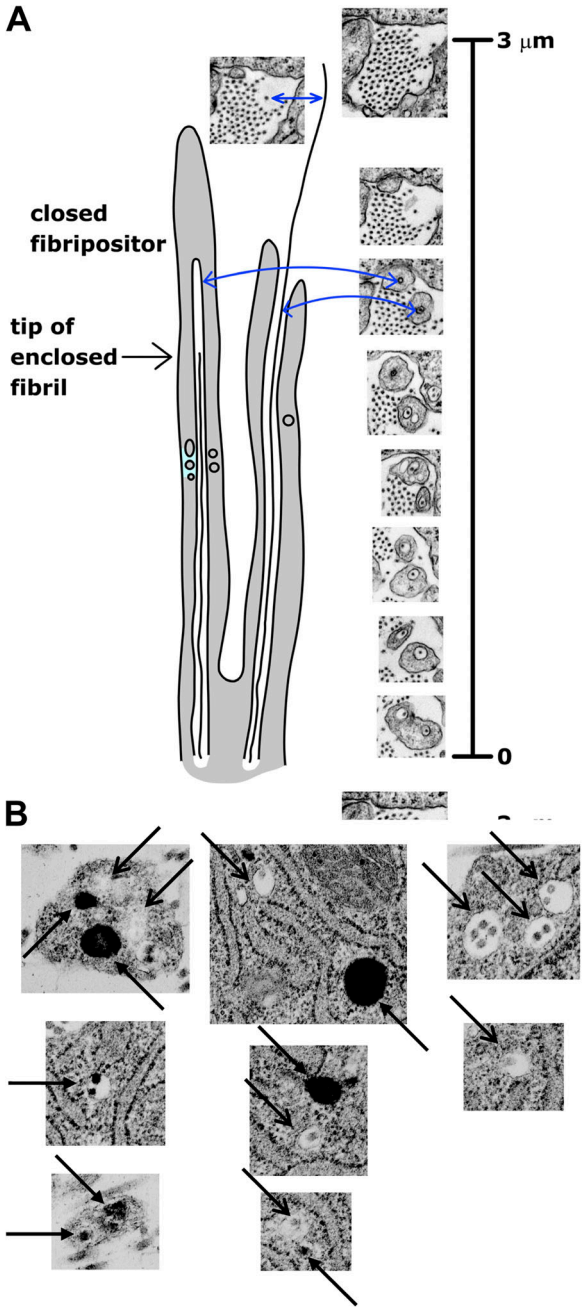

Figure 8. **Fibripositors can be closed at their distal tips.** (A) Transverse sections through a branched fibripositor showing an enclosed GPC^{+cf} (left-hand side arm) and another that is open to the ECM (right-hand side arm). Fibrils are depicted as black lines within the lumen of the fibripositors. Blue arrows point to the same fibril in the electron micrographs and in the schematic. A bar shows the height of the fibripositors. (B) A gallery of electron micrographs in which mouse tail tendons had been treated with HRP and DAB before preparation for EM. Darkly contrasted compartments indicate the presence of HRP (closed arrowhead). Compartments lacking HRP-reactive DAB (simple arrowheads).

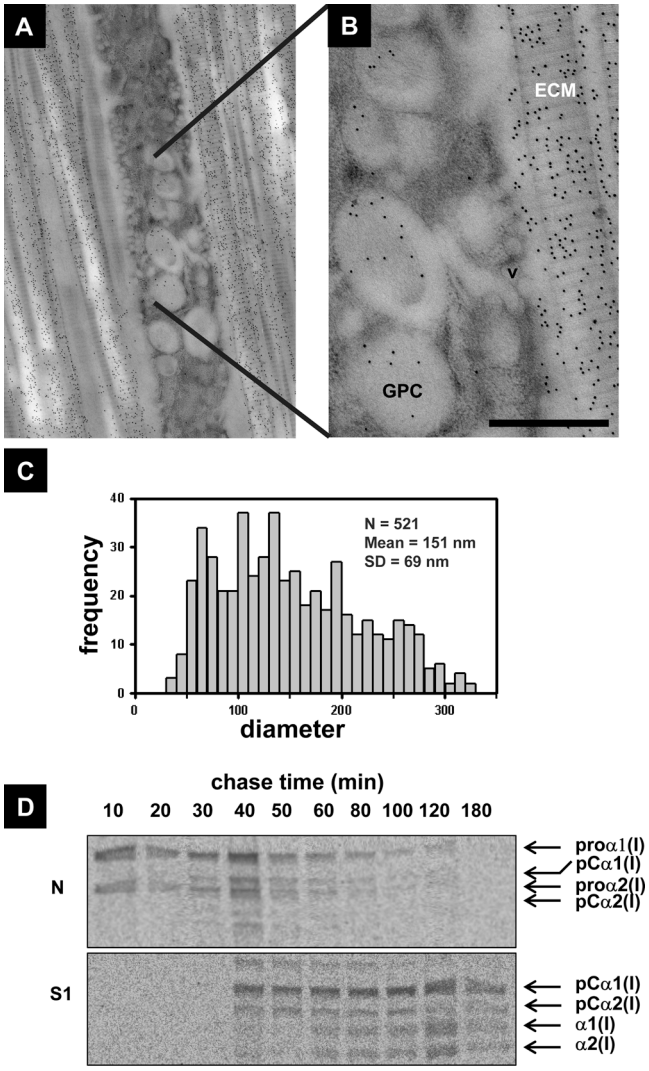

Figure 9. **Fibripositors are absent from 6-wk mouse tail tendon.** (A) Longitudinal section through a mouse tail tendon fibroblast showing a stellate projection surrounded by collagen fibrils. The sample was prepared by high pressure freezing followed by freeze substitution and embedding in LR white. Sections were reacted with a rabbit anticollagen antibody. Secondary antibodies raised to anti–rabbit IgG and conjugated to 10-nm colloidal gold particles reveal the presence of collagen molecules. Posttreated sections were stained with uranyl acetate. (B) Higher magnification of part of the image shown in A. The collagen fibrils in the ECM and the large (~360-nm diam) GPCs were immunoreactive. The small diameter vesicles (v) immediately beneath the PM were not immunoreactive. Bar, 500 nm. (C) Measurement of tail tendon fibril diameters. (D) Tail tendons were incubated in medium containing [^{14}C]proline for 10 min after which the tendons were transferred to medium containing nonlabeled amino acids. At the times indicated the tendons were successively extracted four times in buffer containing NaCl and then a buffer containing NP-40. Autoradiography was used to display the labeled proteins in the chase samples. S1, the first salt extract. N, the NP-40 extract.

No hexagonal packing arrangement was observed presumably because of the heterogeneity in fibril diameters. The cells contained distinct populations of "large" and "small" compartments that had a mean diameter of 361 nm (±22 SEM; n = 210) and 66 nm (±7 SEM; n = 379), respectively (Fig. 9, A and B). The larger compartments were immunoreactive to an anticollagen antibody, and the small compartments were abundant beneath the PM. Analysis of the immunoEM images showed that the large compartments labeled with 35.4 (±2.5 SEM) gold particles per μm^2

whereas the small compartments labeled with 2.0 (±1.1 SEM) gold particles per μm^2. The background labeling within the cell, which included areas of the ER, was 2.3 (±0.4 SEM). Therefore, there was a 17-fold increase in labeling/μm^2 of the large compartments compared with the small compartments. Pulse-chase analysis showed that procollagen and pCcollagen occurred in NP-40–sensitive compartments although pNcollagen and collagen appeared transiently around 40 min of chase. In contrast, the salt extract contained pCcollagen and collagen (Fig. 9 D).

Discussion

Here, we show that in embryonic tendon fibroblasts, (a) procollagen is converted to collagen in the post-Golgi secretory pathway; (b) this collagen assembles into narrow-diameter fibrils within elongated GPCs; (c) the collagen-fibril–containing GPCs ($GPCs^{+cf}$) are targeted to novel PM protrusions, termed fibripositors, that are parallel to the tendon axis; and (d) the lumen of fibripositors open into channels formed between cells to deposit the fibrils into hexagonally packed bundles. Furthermore, fibripositors occur in tendon only during embryonic development when seeding of the ECM occurs; fibripositors are absent during postnatal development despite active procollagen synthesis. Thus, we have identified a novel PM organelle for the ordered assembly of tissues and we have demonstrated a link between the secretory pathway and the synthesis of an organized ECM.

This work has shown that processing of procollagen to collagen begins in Golgi to PM compartments that are refractory to extraction with high salt buffer but which can be solubilized using NP-40 detergent, suggesting that they are within the cell. In addition, we have shown that $GPCs^{+cf}$ are tubular in shape and are completely enclosed within the fibroblast PM. A question of interest is, once $GPCs^{+cf}$ have fused to the PM to form a fibripositor, is the lumen of the fibripositor accessible to salt extraction buffer or does it require NP-40 for solubilization? Incubation of tendons with HRP indicates that diffusion of exogenous molecules (such as trypsin, HRP, and salt ions) into the lumen does occur (Fig. 8 B). Some compartments did not contain DAB-reactive HRP, which is consistent with the presence of $GPCs^{+cf}$ that are enclosed within the cell. It is unlikely that fibripositor lumen close during the extraction process and then become refractory to salt extraction because the compartments that are accessible to salt extraction are also accessible to trypsin (Fig. 2 B). Trypsin digestion was performed directly after labeling and before the salt extractions when tissue shrinkage might be expected to occur. Therefore, it is likely that the material in the NP-40 extract is derived from ER, Golgi, $GPCs^{+cf}$, and potentially from material at the very base of the fibripositor lumen where short early fibrils are found (Fig. 5 B). pNcollagen was absent from the salt extract indicating that the N-propeptides are removed before secretion into the lumen of the fibripositor or ECM and that pCcollagen is the major intermediate used for the extension (embryonic) or broadening (6 wk) of pre-existing fibrils.

Two lines of evidence indicate that collagen fibril polymerization during embryogenesis begins in the TGN or in TGN exit sites, although future studies are needed to identify the origin of collagen-fibril-containing vesicles and precursors of the $GPCs^{+cf}$. First, $GPCs^{+cf}$ near to the Golgi stacks contained cross-banded collagen fibrils. Second, processing of procollagen to collagen was completely prevented in the presence of brefeldin A. The idea that intracellular procollagen processing could be mediated by N- and C-proteinases, which are concomitantly synthesized and trafficked with procollagen is supported by recent work in our laboratory showing intracellular activation of BMP1 in the TGN (Leighton and Kadler, 2003). Cleavage of procollagen would require neutral pH and a concentration of free calcium ions between 2 and 5 mM (Hojima et al., 1985). Alternatively, the procollagen proteinases could be targeted to the ECM and/or the base of the fibripositors and a cycling mechanism, similar to that used by furin (Molloy et al., 1999), could be used to localize the enzymes to the transface of the TGN. Fusion of procollagen containing GPCs with vesicles containing the processing enzymes would then trigger fibrillogenesis and the formation of new $GPCs^{+cf}$.

At 6 wk of development very little cleavage of procollagen to collagen occurs within the cell: the NP-40–soluble compartments contain procollagen and pCcollagen, whereas the NaCl-soluble compartments contain pCcollagen and collagen. No $GPCs^{+cf}$ are observed despite immunolocalization of triple helical collagen to GPCs. Unfortunately, it is not possible to determine which intermediates are present within the GPCs because antibodies that are directed to the collagen triple helix, terminal propeptides, or cleaved neoepitopes will inevitably recognize at least two procollagen intermediates. Further studies are needed to explain the observed difference of N- and C-proteinase activity in embryonic and older tendon fibroblasts. The low abundance and high sequence homology between the various gene products has so far complicated the use of specific antibodies for immunolocalization studies.

Seed and feed mechanism of ECM assembly

Evidence from in vitro studies indicates that collagen fibrillogenesis is a nucleation-propagation process in which the formation of a thermodynamically unstable nucleus occurs slowly but once formed, the nucleus propagates rapidly in size by accretion of collagen molecules (Wood and Keech, 1960; Holmes and Chapman, 1979; Kadler et al., 1987, 1990; Silver et al., 1992). This assembly mechanism predicts the formation of a nucleus having a high fidelity structure because it contains the structural blueprint for the final fibril. The data from embryonic tendon showing the formation of early fibrils at the base of fibripositors, and, the fact that the fibrils exhibit the same diameter as the fibrils in the ECM, are strongly suggestive that a nucleation-propagation assembly mechanism occurs in vivo. An important observation was that fibrils exceeding 10 μm in length could be traced from the center of a fiber bundle within the ECM to the lumen of a fibripositor deep within the cell. There is no evidence that collagen fibrils of this length can be synthesized de novo and deposited whole. Thus, we propose that the nucleation step occurs in GPCs and at the base of the fibripositors, at least in embryonic fibroblasts in situ. Further studies are needed to identify the site of fibril propagation, although the pulse-chase observations of pCcollagen

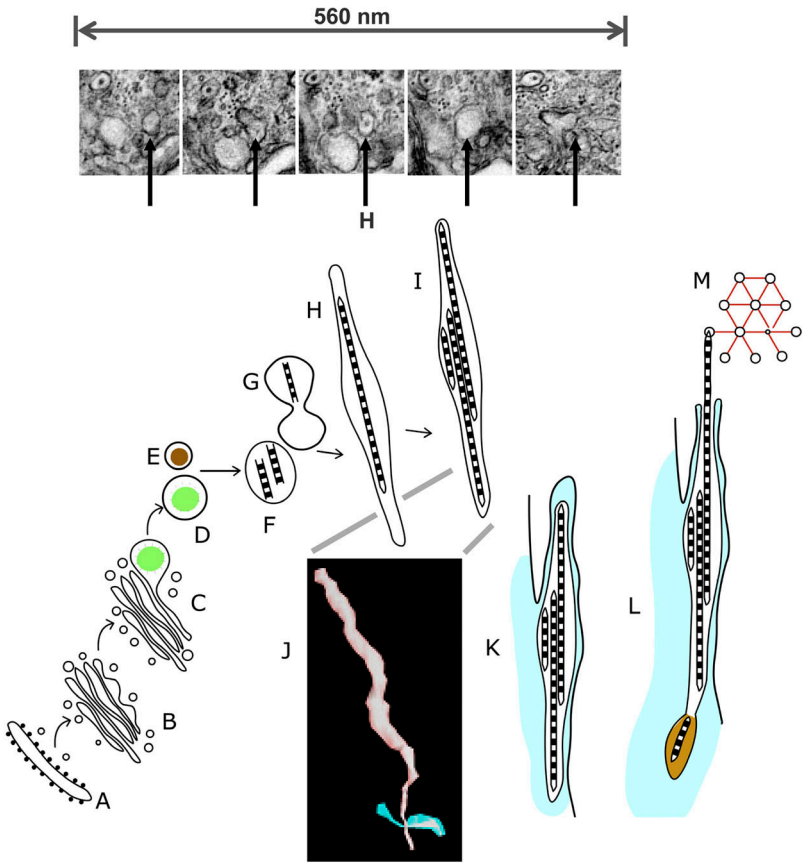

Figure 10. **Proposed biogenesis of fibripositors.** (A) Endoplasmic reticulum; (B) Golgi apparatus; (C) GPCs bud from the trans face of the TGN; (D) GPC containing procollagen; (E) Compartment containing pro–N-/C-proteinases and dibasic proprotein convertases; (F) Cleavage of procollagen to collagen occurs within precursor GPCs^{+cf} to initiate collagen fibril formation; (G) Some GPCs^{+cf} contain a narrow constriction separating two compartments with a collagen fibril in one compartment, as seen in some 3-D reconstructions; (H) GPCs^{+cf} containing a single collagen fibril. Alternate sections through a GPC^{+cf} containing a single fibril are shown (vertical arrows). The ends of the fibril can be seen within the GPC^{+cf}; (I) GPCs^{+cf} containing three collagen fibrils, as seen in some 3-D reconstructions; (J) 3-D reconstruction of a GPC^{+cf}; (K) A GPC^{+cf} pushes out from the PM. The fibripositor is closed, as shown in Fig. 8; (L) A fibripositor delivers a collagen fibril to the ECM where it packs hexagonally into a bundle. Procollagen and the procollagen N- and C-proteinases (ochre) are delivered to the base of a fibripositor where nucleation of collagen fibrils can occur; (M) Schematic of hexagonal packing of collagen fibrils in fibril bundles.

being cleaved to collagen in a NaCl-extractable compartment are consistent with propagation occurring in the ECM or in open fibripositors. The increase in fibril diameter between embryonic and 6-wk stages of development and the subsequent absence of GPCs^{+cf} is consistent with switching off of the nucleation step of fibrillogenesis at postnatal stages (Fig. 10, schematic). The results of immunoEM at 6 wk unequivocally showed the presence of procollagen and/or pCcollagen in ~350-nm-diam compartments, which presumably are responsible for delivering procollagen and pC-collagen to the ECM.

Biogenesis of GPCs^{+cf}, PM channels, and fibripositors

It is a novel observation that procollagen processing can be initiated in the late secretory pathway in vivo. Cultured chick embryo tendon or human fibroblasts secrete procollagen into the cell medium (Jimenez et al., 1971) and procollagen peptidase activity is detected in the medium but not in the cell layer of cultured fibroblasts (Kerwar et al., 1973; Layman and Ross, 1973). In addition, recesses containing collagen fibrils have not been observed in cultured fibroblasts (Birk and Trelstad, 1986), and we have similarly found no evidence of GPCs^{+cf} or fibripositor formation (unpublished data). Cells in culture therefore appear unable to orchestrate the formation of extracellular channels between cells into which parallel collagen fibrils are deposited. This suggests that the parallelism of the tendon is the culmination of the stacking of fibroblasts along the long axis of the tendon, the 3-D organization of the post-Golgi secretory pathway (presumably involving alignment of the cytoskeletal components of adjacent cells) and the extrusion of PM processes into which GPCs^{+cf} are targeted. The intercellular channels appeared to be stabilized by specific points of contact between adjacent cells (Fig. 7 B). The molecular components of these cell–cell contacts remain unknown. Furthermore, the positioning of fibripositors specifically into the intercellular channels presumably involves altered distribution of cell-matrix adhesion molecules, and specific adaptor molecules to ensure fusion of the GPCs^{+cf} only with the distal tip of the fibripositor. Mechanical stimuli might also be expected to influence fibripositor formation, the coalignment of the fibripositors with the ECM, and the directional deposition of collagen fibrils into the ECM. The current work has established a functional link between the post-Golgi secretory pathway and the organization of the ECM and generates a platform for future studies of the cell and molecular basis of tissue assembly.

Perspectives

The 3-D serial section reconstruction studies by Trelstad and colleagues (Trelstad and Hayashi, 1979; Birk and Trelstad, 1984, 1986) in the 1970s and '80s used high voltage transmission electron microscopes to image relatively thick sections. These approaches were so far beyond the technical expertise of most collagen biologists at the time, and the data were so compelling, that few people contemplated extending these studies. However, recent development of state-of-the-art software such as IMOD has made it possible to revisit this approach using larger numbers of thinner sections imaged on a conventional transmission electron microscope.

The results of our work and those obtained by Trelstad, Birk, and colleagues differ in several respects (see references above). First, it was speculated that only uncleaved procollagen was transported to the PM recesses. Our results show that procollagen can be converted to collagen within the cell and that fibril formation can occur in closed intracellular carriers. Furthermore, the recesses were envisioned to broaden at increasing distances from the body of the cell, and it was in these wider zones that fibrils formed into bundles. Our results show that the recesses are long channels in the PM that do not protrude into the cell but run down the surface of the cell. We also show that fibroblasts exhibit fibripositors that are finger-like protrusions from the PM.

Although the study of the cellular aspects of tissue assembly has been simplified by improvements in image analysis software such as IMOD, there remains a major technical hurdle concerning the cells. Fibroblasts flatten when plated out in culture and consequently the PM channels and fibripositors disappear. It is possible to culture whole tendons for up to 3 h and still observe normal procollagen processing but beyond this time the cells lose their embryonic phenotype. Therefore, dissection of the molecular mechanisms involved in PM channel formation and fibripositor biogenesis will rely on the development of novel cell or organ culture methods that preserve the 3-D shape of the cell and provide additional signals needed to specify continued cell differentiation.

Materials and methods

Pulse-chase analysis of procollagen processing in chick embryo tendons

Metatarsal tendons were obtained from day 13 chick embryos. Pulse-chase experiments were performed at 37°C in DME/F12 containing 1% (vol/vol) PS, 2 mM L-glutamine, 200 μM ascorbate, 400 μM βAPN, and supplemented with 2.5 μCi/ml of [^{14}C]proline, 1 mM α,α-dipyridyl or 3.5 μM brefeldin A, as required. Pulse chase was stopped by transferring the tendons to 25 mM EDTA, and 50 mM Tris-HCl, pH 7.5, at 4°C. Trypsin digestion was performed in trypsin-EDTA in HBSS buffer for 30 min at 20°C and control digestions in HBSS buffer alone. For the detection of open fibripositors, tendons were incubated in DME/F12 supplemented with HRP (Sigma-Aldrich) at 37°C for 3 h, fixed with 2.5% glutaraldehyde, and treated with fast DAB (Sigma-Aldrich) before EM analysis. Tendons subjected to pulse-chase analysis in 1 ml aliquots of supplemented medium were extracted in 100 μl aliquots of salt extraction buffer (1 M NaCl, 25 mM EDTA, 50 mM Tris-HCl, pH 7.4) containing protease inhibitors and supplemented as required with 1% NP-40 detergent. Tendons were usually extracted in four changes of salt extraction buffer; overnight (S1), 6 h (S2), overnight (S3), 6 h (S4), and overnight in NaCl extraction buffer containing NP-40 (N). Extracts were analyzed on 4% precast SDS polyacrylamide gels (Invitrogen) under reducing conditions. The gels were fixed in 10% methanol, 10% acetic acid, dried under vacuum, and exposed to a phosphorimaging plate (Fuji BAS-III or BAS-MS). After overnight exposure the phosphorimaging plates were processed using a phosphorimager (Fuji BAS 2000 or 1800).

Protein production, purification, and Western blotting

^{14}C-Labeled procollagen I was purified from human skin fibroblasts as described previously (Kadler et al., 1987). Recombinant human BMP-1 was prepared as described previously (Hartigan et al., 2003). Recombinant ADAMTS-2 was obtained from 293-EBNA cells transfected with a cDNA encoding ADAMTS-2 (a gift from A. Colige, Universite de Liege, Liege, Belgium). Protein extracts were examined by standard Western blot procedures and optimal antibody dilutions determined empirically. Anticalnexin CT, antimembrin and anti-hsp47 antibodies were purchased from StressGen Biotechnologies. Anti-BiP and anticaveolin antibodies were purchased from Santa Cruz. The anti-β1 integrin antibody was from Sigma-Aldrich.

EM

Freshly dissected chick metatarsal tendons were cut into 3-mm lengths and frozen to −196°C using an EM PACT high pressure freezer (Leica). Freeze substitution for ultrastructure was performed using an AFS system (Leica), starting at –90°C in 2% wt/vol osmium tetroxide in actone, going through pure acetone at −50°C and ending in several changes of Spurr's resin (Spurr, 1969). at 20°C. Polymerization in fresh resin was then performed at 60°C for 24 h. Freeze substitution for immunolabeling was performed using an AFS system (Leica) using pure acetone at –90°C, pure ethanol at −50°C in ethanol, and ending in several changes of HM20 Lowicryl resin at −50°C. UV polymerization in fresh resin was then performed at –50°C for 48 h and continued at 20°C for 48 h.

Embryonic mouse tails were fixed in 2% glutaraldehyde in 100 mM phosphate buffer, pH 7.0, for 30 min at RT. The tails were then diced and fixed for 2 h at 4°C in fresh fixative. After washing in 200 mM phosphate buffer they were fixed after in 1% glutaraldehyde and 1% OsO_4 in 50 mM phosphate buffer, pH 6.2, for 40 min at 4°C. After a rinse in distilled water they were en bloc stained with 1% aqueous uranyl acetate for 16 h at 4°C, dehydrated and embedded in Spurrs' resin.

Ultra-thin sections for normal transmission electron microscopy were collected on uncoated copper 200 grids, serial sections for 3-D reconstruction on formvar-coated copper 1,000 μm slot grids (stabilized with carbon film) and ultra-thin sections (~60 nm) for immunolabeling on formvar-coated nickel 400 grids. A postembedding labeling technique was used to detect type I collagen using a rabbit anti–chicken collagen-I antibody (Biodesign International) at a dilution of 1:500 followed by a gold-conjugated goat anti–rabbit antibody (British Biocell International) at a dilution of 1:200. All sections were subsequently stained with uranyl acetate and lead citrate, and examined using either a JEOL 1200EX, Philips EM 400, or Philips BioTwin transmission electron microscope. Images were recorded on 4489 film (Kodak) and scanned using an Imacon Flextight 848 scanner (Precision Camera & Video). Images from EM serial sections were aligned and reconstructed in IMOD for Linux (Kremer et al., 1996) and visualized using OpenSynu for Linux (Hessler et al., 1992).

Online supplemental material

Experimental procedures are available online concerning the differential extraction of secretory pathway proteins and ECM proteins. Fig. S1 depicts the differential extraction of ECM proteins and intracellular proteins. Methods were developed that facilitated the differential extraction of ECM proteins and proteins enclosed within membrane-bound compartments. Proteins in the ECM were solubilized in neutral buffers at 4°C, whereas those in membrane compartments were subsequently extracted in buffers containing NP-40. EM was used to examine the ultrastructure of the cells after each extraction. Western blot analysis was used to examine the protein composition of each extract. Video 1 depicts a 3-D reconstruction of part of a tendon fiber that runs down the mouse tail showing cells and associated fibripositors. Cells are color rendered. Some fibripositors are shown in yellow. The video shows that the cells are cylindrical in shape. Cylindrical channels occur between cells. Online supplemental material is available at http://www.jcb.org/cgi/content/full/jcb.200312071/DC1.

The authors thank Adam Huffman for help and advice with computing, David Mastronarde with help and advise concerning IMOD, Steve Lamont for advice concerning OpenSynu, Alain Colige for the gift of cells expressing recombinant ADAMTS-2, and Gillian Wallis for critical reading of the manuscript.

The work was supported by grants from The Wellcome Trust and the BBSRC (JREI fund), as well as a research collaborative grant from the EU (Framework 5). The EM was carried out in the EM Unit, School of Biological Sciences, University of Manchester, Manchester, UK.

Submitted: 10 December 2003
Accepted: 19 April 2004

References

Birk, D.E., and R.L. Trelstad. 1984. Extracellular compartments in matrix morphogenesis: collagen fibril, bundle, and lamellar formation by corneal fibroblasts. *J. Cell Biol.* 99:2024–2033.

Birk, D.E., and R.L. Trelstad. 1986. Extracellular compartments in tendon morphogenesis: collagen fibril, bundle, and macroaggregate formation. *J. Cell Biol.* 103:231–240.

Bonfanti, L., A.A. Mironov, J.A. Martinez-Menarguez, O. Martella, A. Fusella, M.

Baldassarre, R. Buccione, H.J. Geuze, and A. Luini. 1998. Procollagen traverses the Golgi stack without leaving the lumen of cisternae: evidence for cisternal maturation. *Cell.* 95:993–1003.

Boot-Handford, R.P., D.S. Tuckwell, D.A. Plumb, C.F. Rock, and R. Poulsom. 2003. A novel and highly conserved collagen (pro{alpha}1(XXVII)) with a unique expression pattern and unusual molecular characteristics establishes a new clade within the vertebrate fibrillar collagen family. *J. Biol. Chem.* 278: 31067–31077.

Colige, A., S.W. Li, A.L. Sieron, B.V. Nusgens, D.J. Prockop, and C.M. Lapiere. 1997. cDNA cloning and expression of bovine procollagen I N-proteinase: a new member of the superfamily of zinc-metalloproteinases with binding sites for cells and other matrix components. *Proc. Natl. Acad. Sci. USA.* 94: 2374–2379.

Colige, A., I. Vandenberghe, M. Thiry, C.A. Lambert, J. Van Beeumen, S.W. Li, D.J. Prockop, C.M. Lapiere, and B.V. Nusgens. 2002. Cloning and characterization of ADAMTS-14, a novel ADAMTS displaying high homology with ADAMTS-2 and ADAMTS-3. *J. Biol. Chem.* 277:5756–5766.

Fernandes, R.J., S. Hirohata, J.M. Engle, A. Colige, D.H. Cohn, D.R. Eyre, and S.S. Apte. 2001. Procollagen II amino propeptide processing by ADAMTS-3. Insights on dermatosparaxis. *J. Biol. Chem.* 276:31502–31509.

Graham, H.K., D.F. Holmes, R.B. Watson, and K.E. Kadler. 2000. Identification of collagen fibril fusion during vertebrate tendon morphogenesis. The process relies on unipolar fibrils and is regulated by collagen-proteoglycan interaction. *J. Mol. Biol.* 295:891–902.

Griffiths, G., and K. Simons. 1986. The trans Golgi network: sorting at the exit site of the Golgi complex. *Science.* 234:438–443.

Hartigan, N., L. Garrigue-Antar, and K.E. Kadler. 2003. Bone morphogenetic protein-1 (BMP-1). Identification of the minimal domain structure for procollagen C-proteinase activity. *J. Biol. Chem.* 278:18045–18049.

Hessler, D., S.J. Young, B.O. Carragher, M.E. Martone, S. Lamont, M. Whittaker, R.A. Milligan, E. Masliah, J.E. Hinshaw, and M.H. Ellisman. 1992. Programs for visualization in three-dimensional microscopy. *Neuroimage.* 1:55–67.

Hirschberg, K., C.M. Miller, J. Ellenberg, J.F. Presley, E.D. Siggia, R.D. Phair, and J. Lippincott-Schwartz. 1998. Kinetic analysis of secretory protein traffic and characterization of Golgi to plasma membrane transport intermediates in living cells. *J. Cell Biol.* 143:1485–1503.

Hojima, Y., M. van der Rest, and D.J. Prockop. 1985. Type I procollagen carboxyl-terminal proteinase from chick embryo tendons. Purification and characterization. *J. Biol. Chem.* 260:15996–16003.

Holmes, D.F., and J.A. Chapman. 1979. Axial mass distributions of collagen fibrils grown in vitro: results for the end regions of early fibrils. *Biochem. Biophys. Res. Commun.* 87:993–999.

Jimenez, S.A., P. Dehm, and D.J. Prockop. 1971. Further evidence for a transport form of collagen. Its extrusion and extracellular conversion to tropocollagen in embryonic tendon. *FEBS Lett.* 17:245–248.

Kadler, K.E., Y. Hojima, and D.J. Prockop. 1987. Assembly of collagen fibrils de novo by cleavage of the type I pC-collagen with procollagen C-proteinase. Assay of critical concentration demonstrates that collagen self-assembly is a classical example of an entropy-driven process. *J. Biol. Chem.* 262:15696–15701.

Kadler, K.E., Y. Hojima, and D.J. Prockop. 1990. Collagen fibrils in vitro grow from pointed tips in the C- to N-terminal direction. *Biochem. J.* 268:339–343.

Kadler, K.E., D.F. Holmes, J.A. Trotter, and J.A. Chapman. 1996. Collagen fibril formation. *Biochem. J.* 316(Pt 1):1–11.

Kerwar, S.S., G.J. Cardinale, L.D. Kohn, C.L. Spears, and F.L. Stassen. 1973. Cell-free synthesis of procollagen: L-929 fibroblasts as a cellular model for dermatosparaxis. *Proc. Natl. Acad. Sci. USA.* 70:1378–1382.

Kremer, J.R., D.N. Mastronarde, and J.R. McIntosh. 1996. Computer visualization of three-dimensional image data using IMOD. *J. Struct. Biol.* 116:71–76.

Layman, D.L., and R. Ross. 1973. The production and secretion of procollagen peptidase by human fibroblasts in culture. *Arch. Biochem. Biophys.* 157:451–456.

Leighton, M., and K.E. Kadler. 2003. Paired basic/Furin-like proprotein convertase cleavage of Pro-BMP-1 in the trans-Golgi network. *J. Biol. Chem.* 278: 18478–18484.

Molloy, S.S., E.D. Anderson, F. Jean, and G. Thomas. 1999. Bi-cycling the furin pathway: from TGN localization to pathogen activation and embryogenesis. *Trends Cell Biol.* 9:28–35.

Orci, L., M. Ravazzola, M. Amherdt, A. Perrelet, S.K. Powell, D.L. Quinn, and H.P. Moore. 1987. The trans-most cisternae of the Golgi complex: a compartment for sorting of secretory and plasma membrane proteins. *Cell.* 51: 1039–1051.

Parry, D.A., G.R. Barnes, and A.S. Craig. 1978. A comparison of the size distribution of collagen fibrils in connective tissues as a function of age and a possible relation between fibril size distribution and mechanical properties. *Proc. R. Soc. Lond. B. Biol. Sci.* 203:305–321.

Polishchuk, E.V., A. Di Pentima, A. Luini, and R.S. Polishchuk. 2003. Mechanism of constitutive export from the Golgi: bulk flow via the formation, protrusion, and en bloc cleavage of large trans-Golgi network tubular domains. *Mol. Biol. Cell.* 14:4470–4485.

Polishchuk, R.S., E.V. Polishchuk, P. Marra, S. Alberti, R. Buccione, A. Luini, and A.A. Mironov. 2000. Correlative light-electron microscopy reveals the tubular-saccular ultrastructure of carriers operating between Golgi apparatus and plasma membrane. *J. Cell Biol.* 148:45–58.

Puertollano, R., N.N. van der Wel, L.E. Greene, E. Eisenberg, P.J. Peters, and J.S. Bonifacino. 2003. Morphology and dynamics of clathrin/GGA1-coated carriers budding from the trans-Golgi network. *Mol. Biol. Cell.* 14:1545–1557.

Rambourg, A., Y. Clermont, and L. Hermo. 1979. Three-dimensional architecture of the Golgi apparatus in Sertoli cells of the rat. *Am. J. Anat.* 154:455–476.

Roth, J., D.J. Taatjes, J.M. Lucocq, J. Weinstein, and J.C. Paulson. 1985. Demonstration of an extensive trans-tubular network continuous with the Golgi apparatus stack that may function in glycosylation. *Cell.* 43:287–295.

Sciaky, N., J. Presley, C. Smith, K.J. Zaal, N. Cole, J.E. Moreira, M. Terasaki, E. Siggia, and J. Lippincott-Schwartz. 1997. Golgi tubule traffic and the effects of brefeldin A visualized in living cells. *J. Cell Biol.* 139:1137–1155.

Scott, I.C., I.L. Blitz, W.N. Pappano, Y. Imamura, T.G. Clark, B.M. Steiglitz, C.L. Thomas, S.A. Maas, K. Takahara, K.W. Cho, and D.S. Greenspan. 1999. Mammalian BMP-1/Tolloid-related metalloproteinases, including novel family member mammalian Tolloid-like 2, have differential enzymatic activities and distributions of expression relevant to patterning and skeletogenesis. *Dev. Biol.* 213:283–300.

Silver, D., J. Miller, R. Harrison, and D.J. Prockop. 1992. Helical model of nucleation and propagation to account for the growth of type I collagen fibrils from symmetrical pointed tips: a special example of self-assembly of rod-like monomers. *Proc. Natl. Acad. Sci. USA.* 89:9860–9864.

Spurr, A.R. 1969. A low-viscosity epoxy resin embedding medium for electron microscopy. *J. Ultrastruct. Res.* 26:31–43.

Taatjes, D.J., and J. Roth. 1986. The trans-tubular network of the hepatocyte Golgi apparatus is part of the secretory pathway. *Eur. J. Cell Biol.* 42:344–350.

Thomas, G. 2002. Furin at the cutting edge: from protein traffic to embryogenesis and disease. *Nat. Rev. Mol. Cell Biol.* 3:753–766.

Toomre, D., P. Keller, J. White, J.C. Olivo, and K. Simons. 1999. Dual-color visualization of trans-Golgi network to plasma membrane traffic along microtubules in living cells. *J. Cell Sci.* 112(Pt 1):21–33.

Trelstad, R.L., and K. Hayashi. 1979. Tendon collagen fibrillogenesis: intracellular subassemblies and cell surface changes associated with fibril growth. *Dev. Biol.* 71:228–242.

Wang, W.M., S. Lee, B.M. Steiglitz, I.C. Scott, C.C. Lebares, M.L. Allen, M.C. Brenner, K. Takahara, and D.S. Greenspan. 2003. Transforming growth factor-beta induces secretion of activated ADAMTS-2. A procollagen III N-proteinase. *J. Biol. Chem.* 278:19549–19557.

Wood, G.C., and M.K. Keech. 1960. The formation of fibrils from collagen solutions 1. The effect of experimental conditions: kinetics and electron microscope studies. *Biochem. J.* 75:588–598.